In Vivo Visualization of Vascular Patterns of Rotator Cuff Tears Using Contrast-Enhanced Ultrasound

Tadanao Funakoshi,*† MD, PhD, Norimasa Iwasaki,† MD, PhD, Tamotsu Kamishima,‡ MD, PhD, Mutsumi Nishida,§ PhD, Yoichi Ito,‖ PhD, Makoto Kondo,¶ MD, and Akio Minami,† MD, PhD
Investigation performed at Hokkaido University, Sapporo, Japan

Background: Hypoxia and decreased blood supply have been proposed as risks for tendon rupture. Visualization of the vascularity of intact and torn rotator cuffs would be useful for improving treatments for rotator cuff tear.

Purpose: To assess vascularity inside a tendon or an adjacent rotator cuff insertion point in patients differing in age and extent of damage to the tendon.

Study Design: Cross-sectional study; Level of evidence, 3.

Methods: Ten volunteers (all men) and 15 patients (10 men, 5 women) consented to participate in the study. Contrast agent for enhanced ultrasound was injected intravenously. Enhanced ultrasound images of the torn cuff and the contralateral shoulder were recorded for 1 minute. Four small regions of interest, the articular and bursal sides of the tendon and the medial and lateral sides of the bursa, were studied in all shoulders.

Results: There was a significant decrease in blood flow in the intratendinous region in elderly subjects compared with young subjects, but age had no effect on blood flow in bursal tissue. Blood flow in ruptured rotator cuffs did not differ from that in intact rotator cuffs. The intraclass correlation coefficient for intraobserver reproducibility was 0.82 (95% confidence interval: 0.77-0.86).

Conclusions: The findings of this investigation were the hypovascular pattern in intratendinous tissue compared with the subacromial bursa, the age-related decrease in intratendinous vascularity, and the hypovascular pattern in the tendon, regardless of rupture of the tendon. Clarification of vascular patterns inside or around the torn ends of a rotator cuff will assist in the development of successful treatments for torn rotator cuffs.

Keywords: rotator cuff; contrast-enhanced ultrasound; vascularity; subacromial bursa

The limited healing potential of the ruptured rotator cuff has been documented in an animal model[2] and in human subjects.[8,18] Previous studies have demonstrated that 25% to 90% of repaired rotator cuffs tear again.[3,5,7,9,14] In addition, a recent study suggested that the weakest point after rotator cuff repair using suture anchors was the tendon–suture interface.[3] Hypoxia and decreased blood supply have been proposed as risks for tendon rupture. Kannus and Jozsa[11] reported that degenerative changes, including hypoxic tendinopathy, were associated with spontaneous rupture of the tendon. Yepes et al[24] suggested that hypovascularity determines the site of spontaneous ruptures of the quadriceps. On the basis of these reports, we consider that the high retear rate at the tendon–suture interface may be associated with hypovascularity in the edge of the torn tendon.

Previous studies on rotator cuff vascularity have been conducted using unembalmed cadaveric specimens.[15,19-21] Moseley and Goldie[19] noted a zone of diminished vascularity near the insertion of the supraspinatus. They termed this region the *critical zone* and they believed that it represented an area of anastomosis between the vessels derived from the bone at the point of insertion and the longitudinally directed vessels arising from the arterioles in the muscle belly. Recent histologic investigations demonstrated hypervascularity in the region of the torn edge of the cuff.[6,16,18] However, these methods have inherent limitations such as an in vitro environment, low sensitivity, and qualitative evaluation. Therefore, the microvascular pattern of the rotator cuff in living subjects remains unclear.

*Address correspondence to Tadanao Funakoshi, MD, PhD, Kita 15 Nishi 7, Sapporo, Japan 0608638 (E-mail: tfunakoshi@gmail.com).
†Department of Orthopaedic Surgery, Hokkaido University, Sapporo, Japan.
‡Department of Radiology, Hokkaido University, Sapporo, Japan.
§Diagnostic Center of Sonography, Hokkaido University, Sapporo, Japan.
‖Department of Clinical Trial Management Biostatistics, Hokkaido University, Sapporo, Japan.
¶Memorial Hospital Hokkaido Orthopedics, Sapporo, Japan.

Recent developments in Doppler ultrasound (US) techniques and instruments have improved visualization of small vessels. In addition, microbubble-based US contrast agents have improved visualization of low-volume and slow-flowing vessels by increasing the signal-to-noise ratio. More recent studies have characterized the vascularity of the intact or repaired rotator cuff tendon using contrast-enhanced US (CEUS).[1,4,22] However, the vascularity of the ruptured tendon has not been clarified. In this study, we hypothesized that vascularity inside the tendon or adjacent rotator cuff insertion point changes with age and damage. The objective of this study was to examine differences in microvascularity between the intact cuffs of young and elderly subjects and between intact and ruptured cuffs in the elderly, using CEUS.

MATERIALS AND METHODS

Subjects

This study was approved by the institutional review board of our hospital. Ten volunteers (all men) and 15 patients (10 men and 5 women) consented to participate in the study (Table 1). The criterion for the 15 patients for inclusion in this study was a ruptured supraspinatus tendon on 1 shoulder and a continuous tendon on the contralateral shoulder. Patients with rotator cuff tears on both shoulders or massive tears were excluded from this study. Diabetes, cardiovascular disease, tobacco use, and other vascular conditions were not exclusion criteria. The average age at the time of the US procedure in volunteers and patients was 30.2 ± 3.9 years (mean $\pm$ SD) and 65.7 ± 11.5 years (mean $\pm$ SD), respectively. Fifteen patients underwent MRI for diagnosis before CEUS. Ten patients with rotator cuff tears underwent or were scheduled for surgery for cuff repair because of their symptomatic shoulders. Three patients had a traumatic episode at least 3 months before the US procedure. Shoulders were divided into 4 groups as follows: 10 asymptomatic intact shoulders of young volunteers on the side of the injected arm (INTi group); 10 shoulders of young volunteers contralateral to the injected arm (INTc group); 15 shoulders of patients over 40 years of age with rotator cuff tear (RCT group); and 15 intact shoulders of patients over 40 years of age contralateral to the rotator cuff tear (NRCT group) (Table 1, Figure 1). We used this design to negate any confounding effect of the side on which the contrast agent was injected. The side contralateral to the ruptured rotator cuff was used for the injection in all patients. We compared the INTc group with the RCT group and the INTi group with the NRCT group. On MRI, the mean length of rotator cuff tears was 22.3 mm (range, 10-45 mm), including 2 bursal side partial-thickness tears and 13 full-thickness tears.

Contrast-enhanced US

All US examinations were performed by 1 certified sonographer (M.N.) using an SSA-790A ultrasound unit (AplioXG, Toshiba Medical Systems Corp., Otawara, Japan). The center frequency of the probe was 7.5 MHz. The imaging mode of the CEUS was pulse subtraction.

All scans were done with the shoulder in extension to optimize visualization of the supraspinatus tendon–bone junction (Figure 2). The rotator cuff was imaged in the oblique coronal plane (Figures 3A, 4A, and 5A). A baseline scan was obtained initially to confirm optimum visualization of the intact or ruptured supraspinatus tendon. An intravenous catheter was placed in the left arms of the volunteers and the patients' arms corresponding to the intact tendon. Both shoulders of volunteers and patients underwent lipid microsphere CEUS (Sonazoid, GE Healthcare, Waukesha, Wisconsin).

The contrast agent was injected intravenously at a concentration of 0.015 mL/kg and was followed by a 10-mL saline flush. The CEUS images were recorded for 1 minute after the contrast medium injection. Five minutes after the first injection of contrast medium, the highest mechanical index (1.5) was used to avoid enhancement from previously injected contrast medium. Then the contralateral side was imaged and recorded using the same procedure. No patient experienced adverse events after the injection of contrast medium.

Time–Intensity Curve Analysis of Contrast-Enhanced US

Fifty shoulders were enrolled in this analysis. The stored images were analyzed by the AplioXG-dedicated software ImageLab (Toshiba Medical Systems). It is a prototypal software for research, running on consumer computers, that refers to the internal dynamic range, gain, and the color scale to calculate the precise antilogged values from the images. The regions of interest (ROIs) were identified as 4 circles, 150 ± 10 pixels in area, on the articular side of the tendon (AT), the bursal side of the tendon (BT), the medial side of the bursa (MB), and the lateral side of the bursa (LB). To visualize the vascular pattern in detail, relatively small ROIs were examined intensively using CEUS (Figures 3B, 4B, and 5B).

A vascular signal in the peribursal fat was not included in assessment of the regions of tendons (Figure 3A). A time–intensity curve was measured using an original program (Figures 3C, 4C, and 5C). The data obtained were normalized per shoulder relative to a baseline value using an average from the first 280 frames (about 18 seconds). The values of the area under the time–intensity curve were used for statistical analysis and were expressed as acoustic units. All analyses were performed in a blinded fashion and not in real time by 1 investigator (T.F.). A hypervascular pattern was defined as more than 150 acoustic units, and a hypovascular pattern was defined as less than 100 acoustic units.

Statistical Analysis

All statistical analyses were performed using Excel 2000 (Microsoft Corp., Redmond, Washington) and JMP 8.0

TABLE 1
Characteristics of Patient Data[a]

	Patient Data			Condition of Nonruptured Cuff		Condition of Ruptured Cuff				
No.	Age at Index Surgery (y)	Gender	Injured Side	Cuff Integrity	Pain	Tear Size (mm)	Tear Type	Pain	Treatment	Trauma[b]
1	73	M	R	Heterogeneous	P	30	Full thickness	P	Surgery	Y
2	78	F	L	Heterogeneous	N	40	Full thickness	P	Conservative	N
3	58	M	L	Intact	N	15	Full thickness	P	Conservative	N
4	71	F	R	Heterogeneous	N	10	Full thickness	P	Surgery	N
5	64	F	R	Intact	N	45	Full thickness	P	Conservative	N
6	71	M	R	Intact	N	10	Full thickness	P	Conservative	N
7	60	F	L	Intact	N	25	Full thickness	P	Surgery	N
8	63	M	R	Heterogeneous	P	25	Full thickness	P	Conservative	N
9	80	M	R	Calcification	N	10	BPRCT	P	Surgery	Y
10	80	M	R	Calcification	N	45	Full thickness	P	Surgery	N
11	71	M	R	Intact	N	15	Full thickness	P	Surgery	N
12	58	F	R	Intact	P	20	Full thickness	P	Surgery	N
13	47	F	R	Intact	N	10	BPRCT	P	Surgery	N
14	70	M	L	Intact	N	15	Full thickness	P	Surgery	N
15	41	M	R	Intact	N	20	Full thickness	P	Surgery	Y

[a]Heterogeneous, heterogeneous echo patterns inside the tendon; calcification, calcification inside the tendon; P, pain; N, no pain; BPRCT, bursal-side partial rotator cuff tear.
[b]Trauma: Y, obvious traumatic history; N, no obvious traumatic history.

(SAS Institute, Cary, North Carolina). The means of 2 repeated measurements were used for all analyses. A paired *t* test was used for comparing the means of the INTi and INTc groups and those of the NRCT and RCT groups. An unpaired *t* test was used for comparing the means of the INTi and NRCT groups and those of the INTc and RCT groups. One-way analysis of variance with random effects to accommodate subject variability was used for analysis of area-dependent differences (AT, BT, MB, and LB). A probability of <.05 was considered significant. Linear regression analyses were employed to determine correlations between tear size and acoustic unit in the RCT group. Intraobserver reproducibility was calculated based on 2 consecutive measurements. An intraclass correlation coefficient (ICC) of 1.0 represents perfect agreement, and an ICC of 0 suggests that the measurements are entirely random. The definition of acceptable intraobserver reproducibility depends on the definition of clinical acceptability used in the analysis. In this study, an ICC greater than 0.80 was considered acceptable.

RESULTS

Blood Flow Inside the Supraspinatus Tendon

In all groups, the CEUS procedures showed that the acoustic units inside the supraspinatus tendon were less than 100. These results indicated the presence of a hypovascular pattern inside the supraspinatus tendon. We used time–intensity curve analysis of CEUS in this study. We did not use the number of positive pixels in static "frozen" image, but integral of the increase. Therefore, the static

images, unfortunately, do not illustrate the differences between the images of each group. A comparative study of blood flow differences between the 4 ROIs showed significantly less blood flow inside the supraspinatus tendon (AT and BT) compared with the subacromial bursal tissue (MB and LB) in all groups ($P < .0001$) (Figure 6). There was no significant difference in the vascular distribution inside the supraspinatus tendon (AT vs BT).

Age-Related Differences in Blood Flow in the Intratendinous Region

This analysis revealed that blood flow inside the tendon in the INTi group was higher than that in the NRCT group (AT and BT; $P < .0001$) (Figure 6). One case of an asymptomatic intact tendon in a young volunteer showed a moderate vascular pattern inside the tendon approximately 5 mm from the articular edge of the bone-to-tendon insertion.

Various alterations of the tendon and bursa were observed in the NRCT group: focal swelling of tendons, focal small anechoic lesions at the tendon-to-bone insertion, 2 calcifications, and 4 cases lacking a homogeneous echo pattern in the intratendinous region (Table 1).

Damage-Related Differences in Blood Flow at the Intratendinous Region

There was no significant difference in blood flow inside the tendon between the NRCT and RCT groups (Figure 6). The range of correlation coefficients between tear size and the acoustic unit was −0.394 to 0.454.
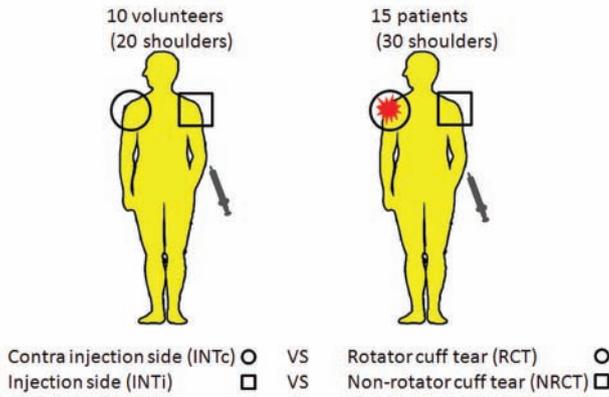
Figure 1. Study design. Shoulders of volunteers contralateral to the injected shoulders were compared with rotator cuff tear shoulders of patients. The injected shoulders of volunteers were compared with the shoulders of patients contralateral to the ruptured rotator cuffs. The red mark indicates a rotator cuff tear.
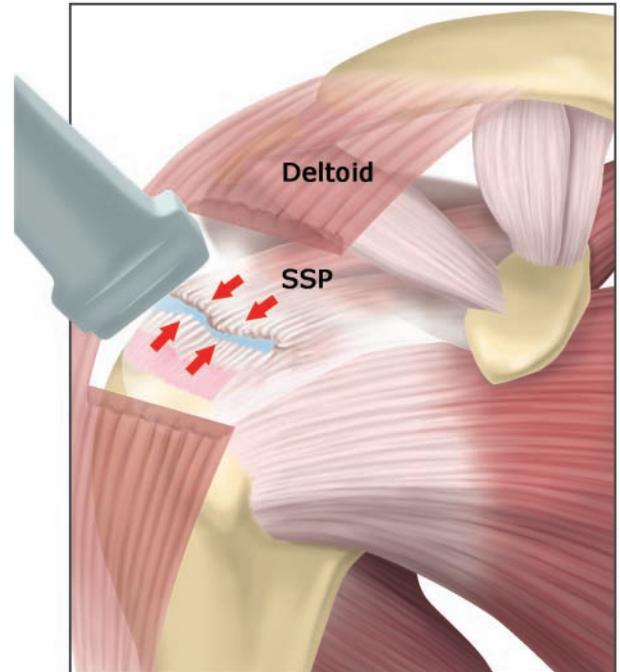
Blood Flow at the Bursal Tissue

Blood flow at the bursal tissue did not differ between the MB and LB regions in any group (Figure 6). A hypervascular pattern in the synovium tissue adjacent to the rotator cuff defect was observed in 4 of the 15 shoulders in the RCT group. The area of high blood flow in the synovium
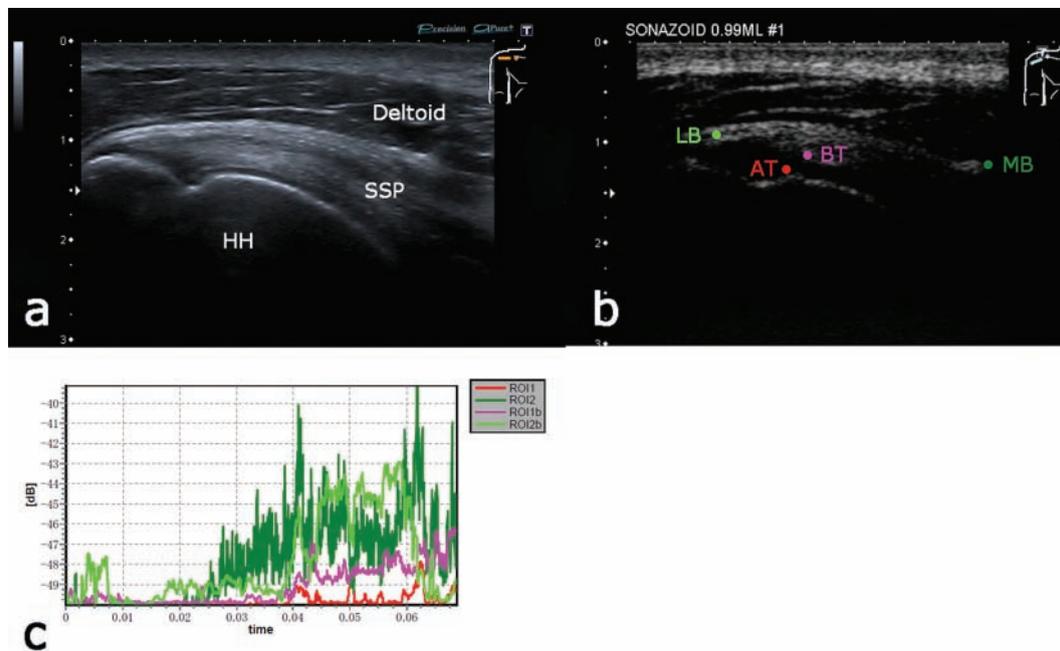

Figure 2. Ultrasound technique used for evaluating rotator cuff tears. The probe was positioned longitudinally to the supraspinatus tendon. Red arrows indicate the ruptured supraspinatus tendon. SSP, supraspinatus tendon; deltoid, deltoid muscle.

Figure 3. Ultrasound of an asymptomatic shoulder of a young volunteer (subject 1 of the INTc group). A, B-mode image; HH, humeral head; SSP, supraspinatus tendon; deltoid, deltoid muscle. B, contrast-enhanced ultrasound (CEUS) image (same plane as for part A). Four regions of interest are shown: AT, articular side of the tendon (red dot); BT, bursal side of the tendon (pink dot); MB, medial side of the bursa (dark green dot); and LB, lateral side of the bursa (light green dot). C, time–intensity curves for each region of interest (ROI) of CEUS.
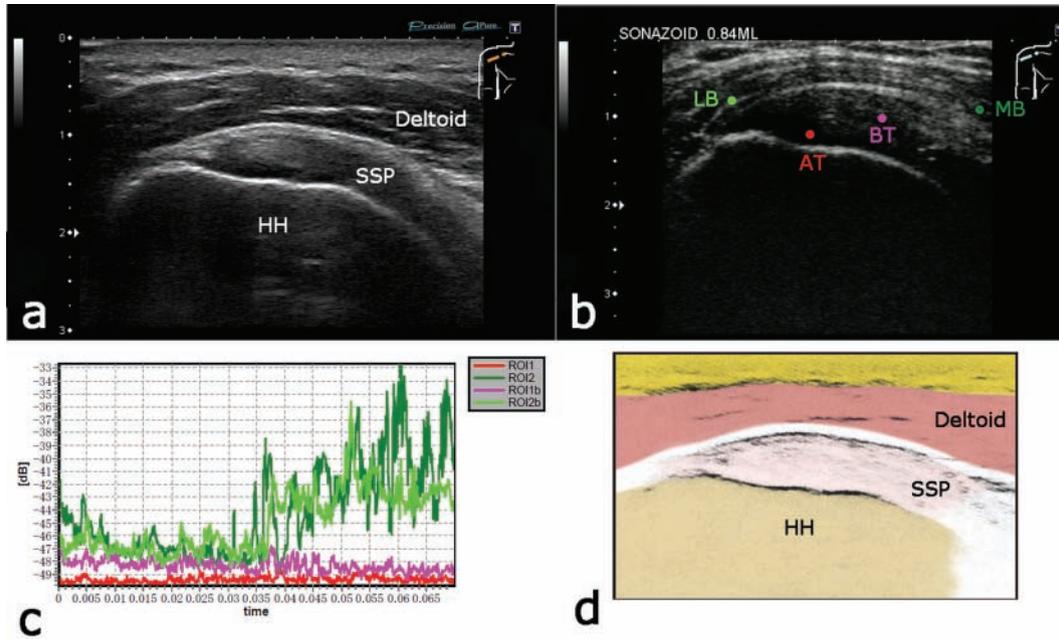
Figure 4. Ultrasound for case 5, intact shoulder (no rotator cuff tear [NRCT]) group. A, B-mode image showing a nonruptured supraspinatus tendon. HH, humeral head; SSP, supraspinatus tendon; deltoid, deltoid muscle. B, contrast-enhanced ultrasound (CEUS) image (same plane as for part A). Four regions of interest are shown: AT, articular side of the tendon (red dot); BT, bursal side of the tendon (pink dot); MB, medial side of the bursa (dark green dot); and LB, lateral side of the bursa (light green dot). C, time–intensity curves for each region of interest (ROI) of CEUS. D, schematic depiction of part A.
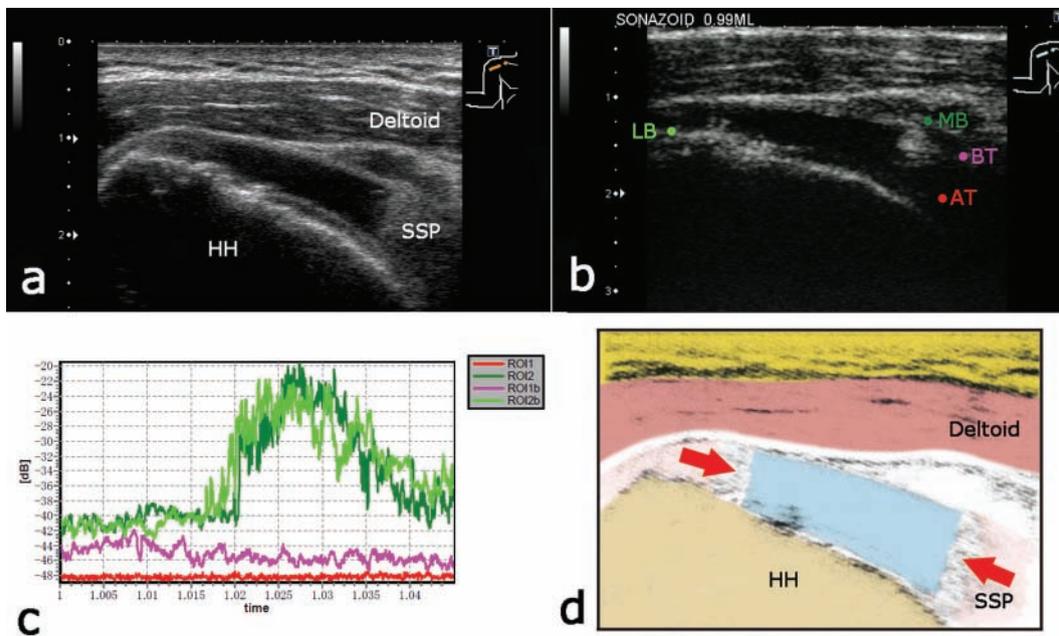

Figure 5. Ultrasound for case 1, rotator cuff tear (RCT) group. A, B-mode image showing a ruptured supraspinatus tendon. HH, humeral head; SSP, supraspinatus tendon; deltoid, deltoid muscle. B, contrast-enhanced ultrasound (CEUS) image (same plane as for part A). Four regions of interest are shown: AT, articular side of the tendon (red dot); BT, bursal side of the tendon (pink dot); MB, medial side of the bursa (dark green dot); and LB, lateral side of the bursa (light green dot). C, time–intensity curves for each region of interest (ROI) of CEUS. D, schematic depiction of part A. The light blue area and the 2 red arrows indicate the ruptured supraspinatus tendon.
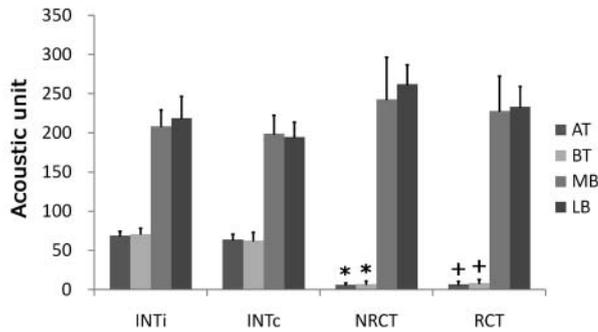
Figure 6. The acoustic units of the area under the time curve were calculated by subtracting the baseline acoustic units from the observed acoustic units for each subject. INTi, injection shoulder of a young volunteer with intact shoulders; INTc, shoulder contralateral to the injection shoulder in a young volunteer with intact shoulders; NRCT, shoulder contralateral to the rotator cuff tear shoulder; RCT, shoulder with a rotator cuff tear. * INTi vs NRCT, $P <$ .0001; [†]INTc vs RCT, $P <$ .0001 (n = 10, INTi and INTc; n = 15, NRCT and RCT).

tissue was not considered part of the tendon in our study and thus did not affect the blood flow value for the tendon in the RCT group.

Age-Related Differences in Blood Flow at the Bursal Tissue

Although an age-related decrease in blood flow was observed for intratendinous tissue, there was no significant difference in blood flow in the bursal tissue between the INTi and NRCT groups (Figure 6); it tended to be higher in the NRCT group than in the INTi group.

Damage-Related Differences at the Bursal Tissue

There was no significant difference in blood flow at the MB and LB between the NRCT and RCT groups (Figure 6). We observed a clear vessel in the MB region, in the peribursal fat about 20 mm from the tendon insertion, in all groups except the RCT group.

Blood Flow Arrival Time

In the young volunteers, the first blood flow was observed in the region of the MB (average, 28.8 seconds). The first blood flow in the NRCT group (average, 24.2 seconds) was observed earlier than in the INTi group in the region of the bursa tissue (P = .0277). There were no differences in blood arrival time between the MB and LB regions. Blood flow in the RCT group had the same tendency as that of the NRCT group. There was no significant difference in blood flow arrival time between the NRCT and RCT groups.

ICC for Intraobserver Reproducibility

The ICC for intraobserver reproducibility was 0.82 (95% confidence interval: 0.77-0.86). The agreement between intraobserver variation for the CEUS analysis and that for the small ROIs was acceptable.

DISCUSSION

The most notable finding of this investigation was the presence of a hypovascular pattern in intratendinous tissue regardless of rupture of the rotator cuff. The other important finding was an age-related decrease in intratendinous vascularity.

Several authors have measured blood flow in musculoskeletal tissue using US.[10,13,23] Using power Doppler US, Silvestri et al[23] revealed that microvessels and vascularity were present in or near the tear. They suggested that blood flow in normal tendons is too weak to be detected by Doppler US.

We were able to measure low rates of blood flow in asymptomatic rotator cuffs using CEUS. The vascularity in the region of the AT and BT was 3 times less than that in the region of the MB in young volunteers. This discrepancy in blood supply between the bursa and tendon is consistent with the hypovascular pattern in the intratendinous region observed in previous histologic analyses.[6,18] The results of our study indicate that a hypovascular pattern is present inside intact and torn cuff tendons. The hypovascular pattern inside the tendon was present in both young and elderly subjects when compared with vascularity in the subacromial bursa. On the other hand, the young group exhibited significantly more vascularity inside the tendon than the elderly group.

Recent studies have demonstrated the feasibility of using CEUS for studying the vascular pattern of the rotator cuff tendon.[4,22] Rudzki et al[22] described vascularity of the supraspinatus tendon and adjacent soft tissue in asymptomatic shoulders. They observed an age-related decrease in the vascular supply of the tendon. Our data also show an age-related decrease in the vascular supply of the intratendinous region. This result is consistent with the limited healing potential of the rotator cuff in the elderly and with better cuff integrity after surgery in the young. On the other hand, Rudzki et al also reported that the articular medial region had consistently less blood supply compared with other regions. However, in our study there was no significant difference in vascularity inside the tendon between the intact rotator cuff and rotator cuff tear groups. This inconsistency may result from differences in size, ROI area, and age. We were able to detect the maximum acoustic unit as well as the time–intensity value of the vascularity pattern. The CEUS images showed that small ROIs are more sensitive to blood flow in small vessels than relatively large ROIs. Therefore, we focused on small ROIs in 4 regions. Although the intratendinous regions of the groups were not of uniform size or shape, the ROIs were set in the same manner.

A vessel adjacent to the rotator cuff in the region of the MB was observed in almost all cases. This vessel was also observed in previous reports.[1] This vessel could be a control vessel because the acoustic values at the MB region were almost the same in the INTi, INTc, and NRCT groups. In the RCT group, this vessel may have shifted proximally as the torn cuff tendon migrated. On the other hand, vascularity in the region of the LB varied between shoulders. The LB region was adjacent to the greater tuberosity in our study. The acoustic values of 2 painful shoulders in the NRCT group, cases 8 and 12, were higher (more than 300 acoustic units) than those of asymptomatic shoulders in the NRCT group. The hypovascularity in the region of the LB may be evidence of a less inflammatory reaction. Recent studies showed that CEUS is a sensitive modality for synovial vascularity evaluations.[12,17] Contrast-enhanced US may be a useful tool for detecting inflammation of the subacromial bursa, which is usually present in clinical conditions such as adhesive capsulitis. There was no significant difference in blood flow at the bursal tissue between the young and elderly groups. However, in light of the age-related decrease in intratendinous tissue, no difference in blood flow in the region of bursa in the elderly group may reflect inflammation or degenerative change. Further studies are required to clarify this issue.

In this study, we focused on the ICC for intraobserver reproducibility because of complications such as the choice of ROIs, adjustment of ROIs to the patient's movement, and normalization. Replication of measurements may reduce the variability inherent to the measurements.

Our study has several limitations. First, normal anatomical structures may cause artifacts with CEUS. In US images of the shoulder, collagen fibers in the tendon appeared either as a dark amorphous area or as a bright area with a fibrillar pattern. The brighter gray scale level may influence the acoustic unit level when the baseline acoustic unit is estimated in the nonenhanced phase. Colored CEUS images would resolve this problem. Second, contrast agent was injected twice during this study. Although the residual contrast agent was enhanced in the second procedure, we considered the amount of residual agent after the first injection insignificant because there was no significant difference between injected and contralateral shoulders (the INTi vs INTc groups). Although we defined hypovascularity as less than 100 acoustic units, many measurements of various tissues would be required to define a standard for vascularity. Moreover, the 4:1 male to female ratio and positioning during the test may have affected the results. An ideal control for vascularity of the torn rotator cuff should be considered. We used the nonruptured rotator cuff as a control. The control group included 3 painful shoulders and 6 with degenerative changes. The contralateral shoulders of a patient with a rotator cuff tear may not be representative of true asymptomatic controls in the same age group.

In conclusion, this investigation revealed a hypovascular pattern in the intratendinous tissue compared with the subacromial bursa and an age-related decrease in intratendinous vascularity in vivo. Moreover, rupture of the rotator cuff did not increase vascularity inside the tendon. Our findings may prove useful for qualitative evaluation of vascularity in tendon-to-bone insertions. When CEUS is used in clinical applications, age-related differences should be taken into account. This novel technique could also be used for determination of intratendinous vascularity before surgery for rotator cuff repair. Although the technique could be developed further, it is currently the best tool for evaluating vascular patterns.

ACKNOWLEDGMENT

REFERENCES

1. Adler RS, Fealy S, Rudzki JR, et al. Rotator cuff in asymptomatic volunteers: contrast-enhanced US depiction of intratendinous and peritendinous vascularity. *Radiology*. 2008;248(3):954-961.
2. Carpenter JE, Thomopoulos S, Flanagan CL, DeBano CM, Soslowsky LJ. Rotator cuff defect healing: a biomechanical and histologic analysis in an animal model. *J Shoulder Elbow Surg*. 1998;7(6):599-605.
3. Cummins CA, Murrell GA. Mode of failure for rotator cuff repair with suture anchors identified at revision surgery. *J Shoulder Elbow Surg*. 2003;12(2):128-133.
4. Gamradt SC, Gallo RA, Adler RS, et al. Vascularity of the supraspinatus tendon three months after repair: characterization using contrast-enhanced ultrasound. *J Shoulder Elbow Surg*. 2009;19(1):73-80.
5. Gerber C, Fuchs B, Hodler J. The results of repair of massive tears of the rotator cuff. *J Bone Joint Surg Am*. 2000;82(4):505-515.
6. Goodmurphy CW, Osborn J, Akesson EJ, Johnson S, Stanescu V, Regan WD. An immunocytochemical analysis of torn rotator cuff tendon taken at the time of repair. *J Shoulder Elbow Surg*. 2003;12(4):368-374.
7. Harryman DT 2nd, Mack LA, Wang KY, Jackins SE, Richardson ML, Matsen FA 3rd. Repairs of the rotator cuff: correlation of functional results with integrity of the cuff. *J Bone Joint Surg Am*. 1991;73(7):982-989.
8. Hawkins RJ, Misamore GW, Hobeika PE. Surgery for full-thickness rotator-cuff tears. *J Bone Joint Surg Am*. 1985;67(9):1349-1355.
9. Jost B, Zumstein M, Pfirrmann CW, Gerber C. Long-term outcome after structural failure of rotator cuff repairs. *J Bone Joint Surg Am*. 2006;88(3):472-479.
10. Kamishima T, Tanimura K, Henmi M, et al. Power Doppler ultrasound of rheumatoid synovitis: quantification of vascular signal and analysis of interobserver variability. *Skeletal Radiol*. 2009;38(5):467-472.
11. Kannus P, Jozsa L. Histopathological changes preceding spontaneous rupture of a tendon: a controlled study of 891 patients. *J Bone Joint Surg Am*. 1991;73(10):1507-1525.
12. Lee SH, Suh JS, Shin MJ, Kim SM, Kim N, Suh SH. Quantitative assessment of synovial vascularity using contrast-enhanced power Doppler ultrasonography: correlation with histologic findings and MR imaging findings in arthritic rabbit knee model. *Korean J Radiol*. 2008;9(1):45-53.
13. Levy O, Relwani J, Zaman T, Even T, Venkateswaran B, Copeland S. Measurement of blood flow in the rotator cuff using laser Doppler flowmetry. *J Bone Joint Surg Br*. 2008;90(7):893-898.
14. Liu SH, Baker CL. Arthroscopically assisted rotator cuff repair: correlation of functional results with integrity of the cuff. *Arthroscopy*. 1994;10(1):54-60.
15. Lohr JF, Uhthoff HK. The microvascular pattern of the supraspinatus tendon. *Clin Orthop Relat Res*. 1990;254:35-38.

16. Longo UG, Franceschi F, Ruzzini L, et al. Histopathology of the supraspinatus tendon in rotator cuff tears. *Am J Sports Med*. 2008;36(3):533-538.

17. Magarelli N, Guglielmi G, Di Matteo L, Tartaro A, Mattei PA, Bonomo L. Diagnostic utility of an echo-contrast agent in patients with synovitis using power Doppler ultrasound: a preliminary study with comparison to contrast-enhanced MRI. *Eur Radiol*. 2001;11(6): 1039-1046.

18. Matthews TJ, Hand GC, Rees JL, Athanasou NA, Carr AJ. Pathology of the torn rotator cuff tendon: reduction in potential for repair as tear size increases. *J Bone Joint Surg Br*. 2006;88(4): 489-495.

19. Moseley HF, Goldie I. The arterial pattern of the rotator cuff of the shoulder. *J Bone Joint Surg Br*. 1963;45:780-789.

20. Rathbun JB, Macnab I. The microvascular pattern of the rotator cuff. *J Bone Joint Surg Br*. 1970;52(3):540-553.

21. Rothman RH, Parke WW. The vascular anatomy of the rotator cuff. *Clin Orthop Relat Res*. 1965;41:176-186.

22. Rudzki JR, Adler RS, Warren RF, et al. Contrast-enhanced ultrasound characterization of the vascularity of the rotator cuff tendon: age- and activity-related changes in the intact asymptomatic rotator cuff. *J Shoulder Elbow Surg*. 2008;17(1 suppl):96S-100S.

23. Silvestri E, Biggi E, Molfetta L, Avanzino C, La Paglia E, Garlaschi G. Power Doppler analysis of tendon vascularization. *Int J Tissue React*. 2003;25(4):149-158.

24. Yepes H, Tang M, Morris SF, Stanish WD. Relationship between hypovascular zones and patterns of ruptures of the quadriceps tendon. *J Bone Joint Surg Am*. 2008;90(10):2135-2141.